Revista Mexicana de Astronomía y Astrofísica
Universidad Nacional Autónoma de México
rmaa@astroscu.unam.mx
ISSN (Versión impresa): 0185-1101
MÉXICO

2005
Margarita Rosado
SOME ASTRONOMICAL NICHES WITH 3D SPECTROSCOPY
Revista Mexicana de Astronomía y Astrofísica, diciembre, año/vol. 024
Universidad Nacional Autónoma de México
Distrito Federal, México
pp. 92-101

RevMexAA (Serie de Conferencias), **24**, 92–101 (2005)

SOME ASTRONOMICAL NICHES WITH 3D SPECTROSCOPY

Margarita Rosado[1]

RESUMEN

Se presenta un panorama de algunos de los resultados más interesantes obtenidos con espectrómetros 3D en telescopios de $\sim$ 4m de diámetro con la intención de aprovechar estas experiencias en la definición de programas científicos con telescopios de gran diámetro como el GTC.

ABSTRACT

An overview of some of the most interesting results obtained with the use of 3D spectrometers working in 4m-class telescopes is given with the purpose of taking advantage of those experiences in the definition of scientific programs for telescopes of larger diameter as the GTC.

Key Words: **COSMOLOGY: DARK MATTER — GALAXIES: INTERACTIONS — GALAXIES: KINEMATICS AND DYNAMICS — INSTRUMENTATION: SPECTROGRAPHS — ISM: KINEMATICS AND DYNAMICS**

1. INTRODUCTION

3D spectrographs are instruments that provide spectra at each pixel over the whole field of view (FOV) of the instrument. In order to achieve this, 3D instruments are built with two esential components of high optical quality: a collimator and a camera. Both the collimator and camera should be qualified to give good images over the entire FOV. Several additional components could be placed at two main locations: the focal plane and within the collimated beam (i.e., the place between the collimator and the camera). The addition of different components at those locations defines the type of 3D spectrograph. For example, an *imager* has, in addition to the basic collimator+camera system, an interference filter wheel at the focal plane (or within the collimated beam); what is called a *Fabry-Perot interferometer* has, in addition to the basic system, a wheel with interference filters at the focal plane and a scanning Fabry-Perot (FP) interferometer within the collimated beam; a *TIGER-type* instrument has, in addition to the collimator+camera system, an enlarger, a field lense, and an array of microlenses at the focal plane, whereas, within the collimated beam, a grism is placed; a *PHYTEAS-type* instrument has the same components that a *TIGER-type* instrument with the addition of a scanning FP interferometer within the collimated beam; *MOS* instruments (multiple object spectroscopy) have the two main components and a multi-slit at the focal plane and a grism within the collimated beam.

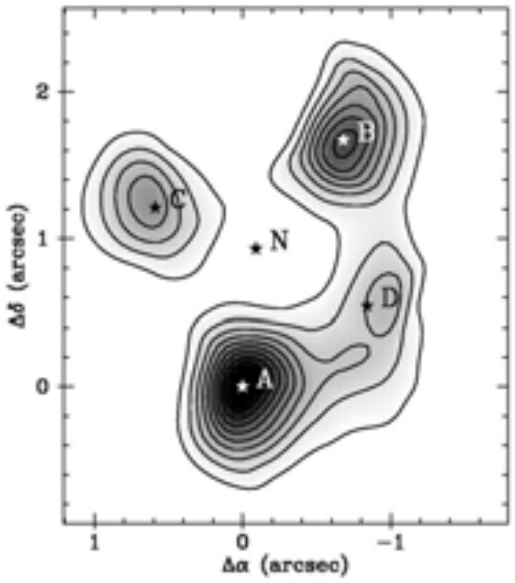

Fig. 1. INTEGRAL CIII] emission of the Einstein Cross. From Mediavilla et al. (1998).

The several components and their combinations give rise to a large variety of 3D spectrometers that could be used to study different astronomical phenomena (see Connes & Le Coarer 1995). Though, in the conception, they share the main components in common, in practice, it is quite difficult to construct 3D spectrometers capable of implementing more than two or three different modes. Indeed, it is recommended to build dedicated instruments that use, in the more efficient way, one or two of the capabilities of 3D spectroscopy.

[1]Instituto de Astronomía, UNAM, México.

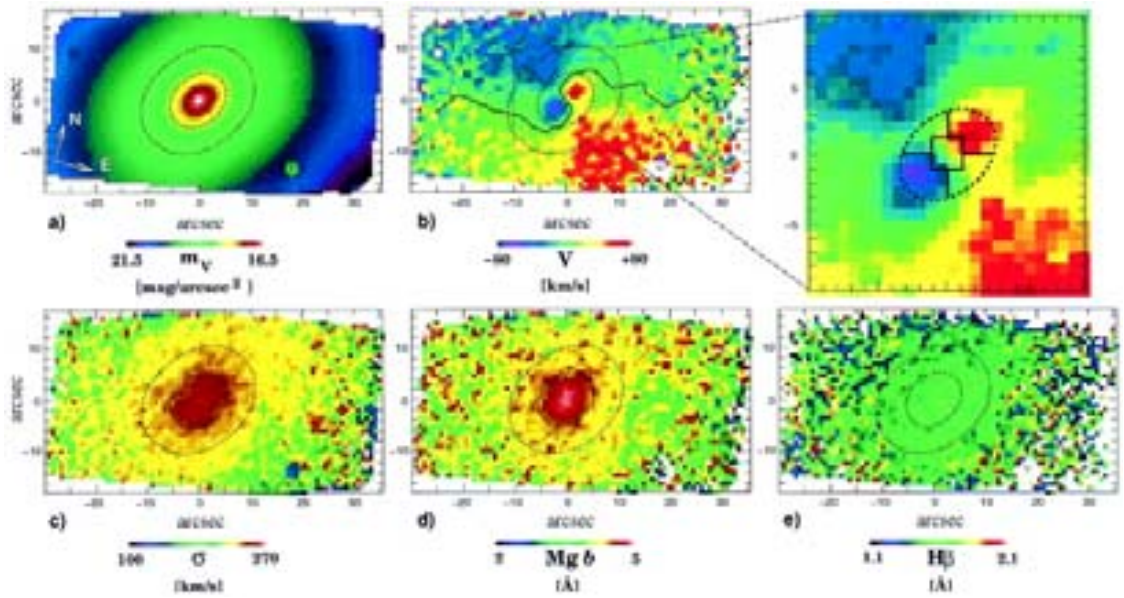

Fig. 2. SAURON observations of the E3 galaxy NGC 4365. From left to right: (a) continuum visual magnitude. (b) stellar mean velocity, V and, to the right, a close-up of the central part. (c) Stellar velocity dispersion. (d) Mg index. (e) Hβ index. From de Zeeuw et al. (2002).

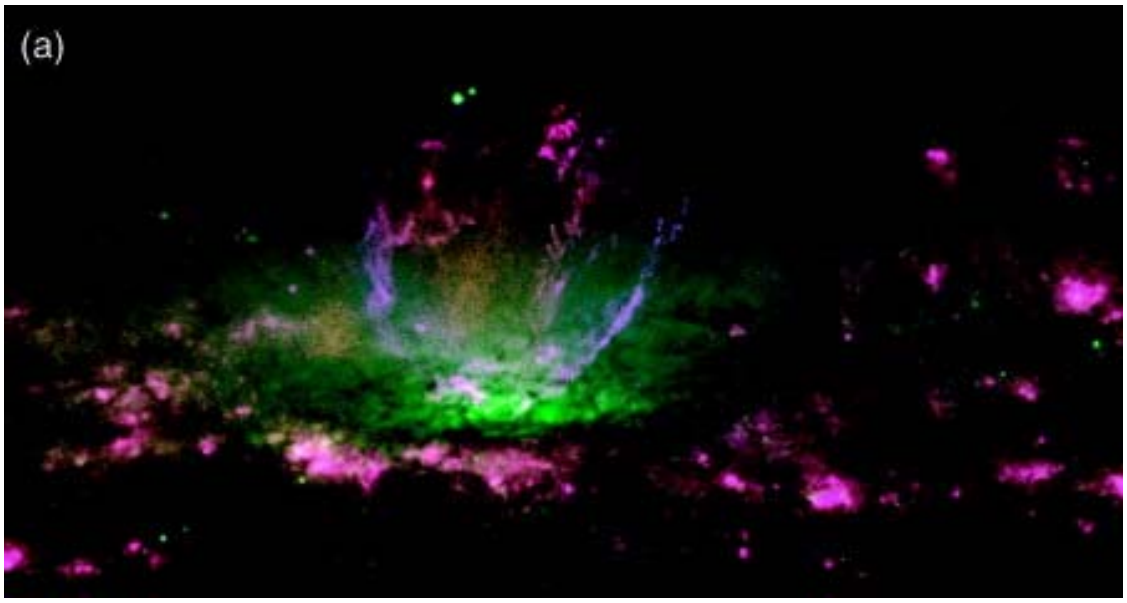

Fig. 3. Composite image of the superbubble in NGC 3079. Green: I-band continuum. Red: Hα. Blue: [NII]. From Cecil et al. (2001).

3D spectrometers give, at once, huge spectral information of extended sources and that is why their use is the most efficient for large diameter telescopes. Besides, when using 3D spectrometers, several practical problems presented during observations disappear: precise pointing of the sources, identification of the regions where the spectra has been obtained, to cite some of them.

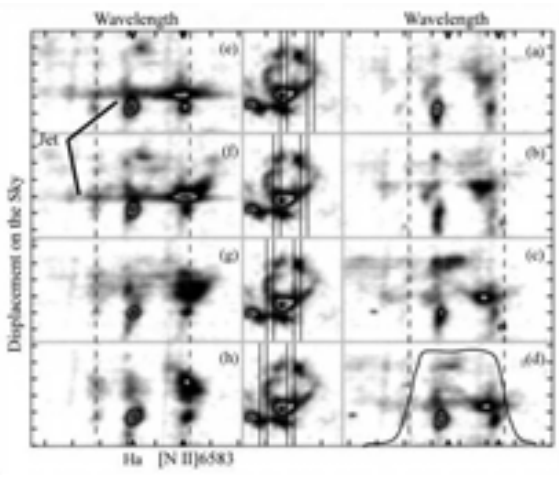

Fig. 4. Position-velocity diagrams constructed from FP data cubes of the superbubble emission in NGC 3079. The central panels indicate the positions over the superbubble used to integrate the position-velocity diagrams. Note the complex velocities across the superbubble that blend the Hα and [NII] lines. From Cecil et al. (2001).

This kind of instruments are ideal for studying collections of point-like objects spread over large fields, or asymmetrical extended objects where the classical long-slit spectrometers do not give the complete information required to do the job. In addition, 3D spectrometers are the only instruments well suited to really take advantage of adaptive optics because they do not degrade the high image quality furnished by adaptive optics systems.

There are two main types of 3D instruments that are being used extensively:

– *IFU-type*

and

– *Fabry-Perot type*

IFU-type instruments (for Integral Field Units) are 3D spectrometers that use grisms within the collimated beam and microlenses arrays or optical fiber bundles at the focal plane. Although all the 3D spectrometers can be considered as Integral Field Spectrometers, it is common to associate this name with this particular mode of 3D spectroscopy. Some examples of *IFU-type* instruments are TIGER, OASIS, SAURON and INTEGRAL, amongst others. This type of instruments typically provide moderate spectral resolutions, R$\sim$ 5000, high spatial resolution (limited by telescope's capabilities) and a small FOV ($\sim 20\,''$). A great success of this type of instruments is that they work both with emission and absorption lines. Thus, this kind of instruments could provide spectra of both gas and stars.

Fabry-Perot type instruments are those 3D spectrometers that use scanning FP interferometers within the collimated beam and interference filters either at the focal plane or within the collimated beam. Some examples of *Fabry-Perot type* instruments are: CIGALE, HiFi, RUTGERS, PUMA and TTF, to cite some of them. They typically provide relatively high spectral resolutions, R$\sim$ 20000, moderate spatial resolution and a large FOV ($\sim$ 10 – $20'$). In general, this type of instruments work with emission lines although, in principle, their use can be extended to absorption lines.

In what follows, I will present some of the most interesting results obtained with 3D spectrometers of the types defined above used in 4m-class telescopes. The aim of this work is to present an overview of the problems that have been tackled successfully with 3D spectrometers. Some of these problems are now astronomical niches.

2. SCIENTIFIC DRIVERS OF IFU OBSERVATIONS

2.1. *Black hole mass determinations in the centers of galaxies*

A good example of the achievements done with *IFU-type* instruments is given in Emsellem et al. (1999). In that work, HST photometry and ground-based kinematical observations are presented for the S0 galaxy NGC 3115. The kinematics were obtained using the prototype of *IFU-type* instruments, TIGER, at the Canada-France-Hawaii Telescope (CFHT). TIGER data consisted in more than 600 stellar spectra of spectral resolution of 3.7 Åpixel^{-1} and spatial resolution of $0''.39$ over a FOV of $14''.5 \times 7''.9$ covering the very center of this galaxy suspected to host a black hole. From the spectra, the authors were able of constructing the 2D Gauss-Hermite moments: V (velocity), σ_V (velocity dispersion), h_3 and h_4. Combining the stellar kinematics with the photometry and modeling the photometry with the Multiple Gaussian Expansion technique, it was possible to show that the kinematics were well fitted with a two-integral Jeans model implying a central dark mass $M_{BH} \geq 6.5 \times 10^8$ M$\odot$.

2.2. *Detection of an arc of extended emission in the Einstein Cross*

Figure 1 depicts the redshifted emission at CIII] (λ 1909 Å) of the Einstein Cross, obtained from the 2D spectra of INTEGRAL at the William Hershel Telescope at Canary Islands (WHT; Mediavilla et al. 1998). This instrument is of the *IFU-type* and works with an optical fiber system instead of the microlenses array of other IFUs.

The Einstein Cross is a gravitational lens system constituted of four components that appear clearly separated in the continuum intensity map. However, in the CIII] emission line, it exhibits an arc of extended emission connecting the components A, B and D. This connection has been interpreted as a gravitational lens image of the extended narrow line region of a compact source. The compact source itself forms, in turn, the continuum-light gravitational lens image. Applying a lens model that consists of a compact source plus an extended region it is possible to reproduce the arc. In this way, Mediavilla and collaborators were able of estimating the dimensions of the narrow line region of this source, being of about 400 h^{-1} pc.

2.3. *The SAURON Survey*

This survey (Bacon et al. 2001, de Zeeuw et al. 2002) is aimed at determining the intrinsic shapes of early-type galaxies as well as their orbital structure, the mass-to-light ratio as a function of radius, the age and metallicity of the stellar populations, and the frequency of kinematically decoupled cores and nuclear black holes. It is currently conducted using the SAURON instrument attached to the WHT. The SAURON instrument is based on the prototypical integral field spectrometer TIGER (as described in the Introduction and in Section 2.1). SAURON gives spectra, in its low resolution mode, with spectral resolution of 3.6 Å over a FOV of $33'' \times 41''$, sampled with $0''.94 \times 0''.94$ pixels, while in its high resolution mode, the spectral resolution is 2.8 Å , in a FOV of $9'' \times 11''$, sampled with $0''.27 \times 0''.27$ pixels. The working wavelength range of this instrument is 4810 – 5350 Å, covering the wavelengths of the Mg b triplet and Fe lines, for stellar kinematics, as well as the [OIII] (λ 4959 and 5007 Å) and Hβ emission lines, for gas kinematics.

In Figure 2 are shown 2D photometric and kinematic data of both gas and stars in the central region of the E3 galaxy NGC 4365. These data illustrates what is called a decoupled core: while the main body of this galaxy rotates around the projected major axis, the core rotates around the minor axis. This, together with the misalignment between the kinematic and photometric axis of the main body, are strong indications of a triaxial intrinsic shape and that the galaxy underwent a sequence of mergers.

3. SCIENTIFIC ACHIEVEMENTS OF *FABRY-PEROT TYPE* OBSERVATIONS

3.1. *Search for starburst driven galactic winds*

The detection of starburst driven galactic winds has been quite successful by means of observations with FP interferometers. This has been done mainly with the FP instruments HiFi, working at the CFHT and TAURUS-II working at the WHT. It is now known from these observations, that several galaxies show strong and high speed winds, as for example, NGC 3079 (Veilleux et al. 1995, Cecil et al. 2001) and, more recently, NGC 4631 (Melo et al. 2003).

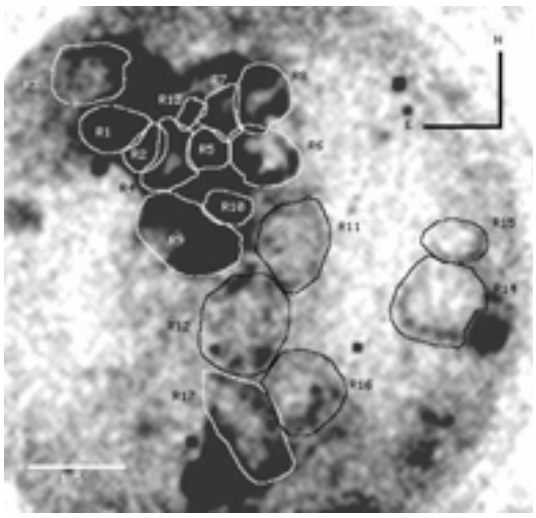

Fig. 5. PUMA velocity map (at $V_{HELIO} = -234$ km s^{-1}) of the Hα emission of the irregular galaxy IC 1613. Superimposed on this map are the boundaries of 17 superbubbles detected in this galaxy (from Valdez-Gutiérrez et al. 2001).

Although the image is quite well known, Figure 3 shows the huge extent of the winds ejected from the nucleus of the galaxy NGC 3079. In this spectacular image, it is seen a 40 $''$ ($\sim$ 3 kpc) wide concave open superbubble having its base at the nucleus of NGC 3079. Figure 4 shows some of the position-velocity diagrams obtained from the FP emission-line profiles at Hα, [NII] (λ 6548 Å) and [NII] (λ 6584 Å). The FP data cover more than $4'.6$ across the galaxy and have a spatial sampling of $0''.67$. The velocity resolution is 70 km s^{-1}. Figure 4 shows the complex velocity profiles across the nuclear superbubble and other regions in this galaxy that imply winds of hundredths of km s^{-1} at galactic scale-lengths. It is not yet sure whether the gaseous flow could scape from the galaxy but at least, it energizes large amounts of the disk and extraplanar zones.

The discovery of galactic winds in starburst galaxies in now being studied extensively by means of a new technique: *excitation maps*, implemented with tunable filters (see Veilleux this meeting). This kind of research could be done with the OSIRIS tunable filters at the GTC. By means of these studies

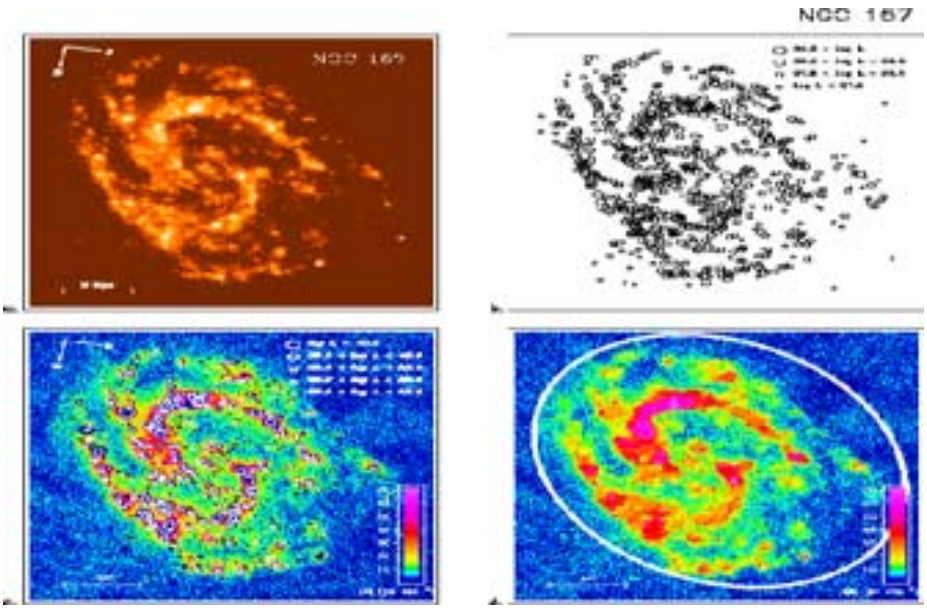

Fig. 6. (a) Hα continuum-subtracted image of NGC 157. (b) Positions of the catalogued HII regions. (c) Hα diffuse emission obtained after subtracting the catalogued HII regions. (d) Upper-limit DIG map. From Zurita et al. (2000).

it would be possible to establish the conditions required to trigger these winds.

3.2. *Superbubble kinematics in the irregular galaxy IC 1613*

Figure 5 shows how the wind-blown bubbles can modify the interstellar medium (ISM) of an entire galaxy. Indeed, Valdez-Gutiérrez et al. (2001) have found that the ionized ISM of the irregular galaxy IC 1613 is completely pierced by several expanding superbubbles (diameters $\leq$ 500 pc and expansion velocities up to 50 km s^{-1}), formed by the winds and supernova explosions of the interior stellar associations. Furthermore, young stellar associations are located at the superbubbles' boundaries suggesting that shock-induced star formation works in this galaxy (Rosado et al. 2002). This kind of studies allows us to know the interplay between massive stars and gas in galaxies. The kinematic data were obtained by means of the PUMA instrument at the 2.1m telescope of the Observatorio Astronómico Nacional at San Pedro Mártir, B.C., México (OAN). PUMA provides a FOV of 10 $'$ with a spatial sampling of 0$''$.59 and a sampling velocity resolution of 20 km s^{-1}.

3.3. *Detection of diffuse ionized gas in galaxies*

Since the seminal discovery of diffuse ionized gas (DIG) at high heights above the Galactic Plane by means of FP interferometry (see a review in Reynolds 2002), this component, whose source of excitation is not yet understood, has been detected in other galaxies as well. Curiously enough, the detection of DIG in other galaxies is being done by means of imaging, both with classical interference filters (Rand 1996) or, more recently, with the Taurus Tunable Filters (Miller & Veilleux 2003). There are a number of edge-on galaxies where extraplanar DIG (e-DIG) is being discovered. Edge-on galaxies are the most favorable case for such detections by means of imaging. However, detecting the DIG in less inclined galaxies is important both, to know more about this component, as well as to subtract it to the HII region intensities of the disks. The identification of DIG in this latter case could be achieved with imaging while the obtention of its kinematics is better done by using FP spectrometers.

Figure 6 from Zurita et al. (2000) exemplifies how the DIG component in the galaxy NGC 157 can be extracted from the total Hα emission of the disk that contains bright emitting HII regions. The results show a good correlation between the high DIG intensities and the most luminous HII regions indicating that the DIG in this case is located at the disk of the galaxy. This correlation also suggests that the source of ionization of the DIG in NGC 157 is connected with the photoionizing flux of OB stars in this galaxy.

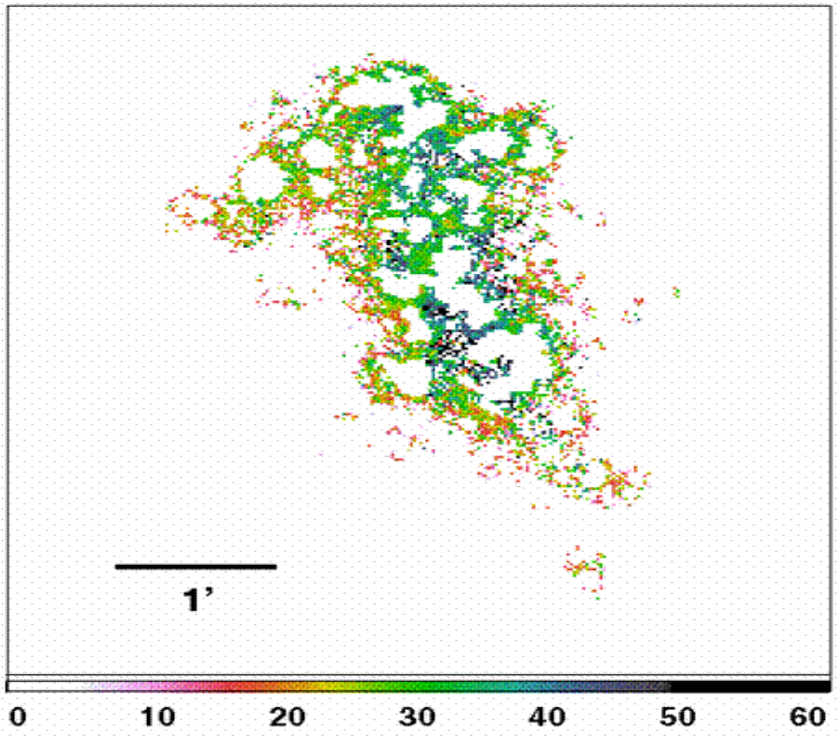

Fig. 7. Velocity dispersion map of the DIG in the irregular galaxy NGC 4449 obtained from PUMA FP spectroscopy. From Valdez-Gutiérrez et al. (2002).

DIG kinematics is an important issue that can throw light on the origin of this component. Figure 7 shows the velocity dispersions of the DIG in the irregular galaxy NGC 4449 (Valdez-Gutiérrez et al. 2002). These kinematic data were obtained using the PUMA Fabry-Perot interferometer at the OAN. One important result is that DIG velocity dispersions are larger than the velocity dispersions of HII regions in this galaxy. Furthermore, it shows that DIG velocity dispersions imply supersonic motions suggesting that shocks are present and should be taken into account in the excitation of the DIG, at least for this galaxy.

3.4. *Low surface brightness galaxies and their dark matter halo distributions*

Low surface brightness galaxies (LSBGs) and dwarf galaxies seem to be almost formed of dark matter (DM) haloes. However, the rotation curves of LSBGs derived from HI kinematics or optical long-slit spectroscopy do not confirm the central DM distribution predicted from models of cold DM (CDM). There is still a fruitful controversy about this issue that has conducted to a revision of both the models and the observational data. In order to settle this controversy it is necessary to obtain 2D high spatial and spectral resolution spectra of the central regions of LSBGs, both for stars and gas. Thus, this controversy could be solved by means of the use of 3D spectrometers both *IFU-type* and *Fabry-Perot type*.

FP interferometers have longtime been used to obtain rotation curves of galaxies for they provide velocity fields with good spatial and spectral resolution, from which the rotation center and the major axis position can be determined. Using a FP at the CFHT, providing good spatial sampling and a spectral resolution of about 20 km s^{-1}, Blais-Ouellette et al. (2001) extracted the rotation curves of two irregular dwarf galaxies from the 2D velocity fields. Figure 8 shows the fits that Blais-Ouellette and collaborators have done for the rotation curve of NGC 3109. Different DM halo distributions (amongst others, pseudoisothermal and CDM) have been fitted to the observed rotation curve and they found that the cuspy DM haloes predicted by CDM scenarios are not well fitted to the data.

Furthermore, using the *IFU-type* SparsePak instrument at the WYN telescope, Swaters et al. (2003) obtained the 2D velocity field of the central region ($72'' \times 72''$) of the LSBG DDO 39, with a velocity resolution of 66 km s^{-1}. The authors report the

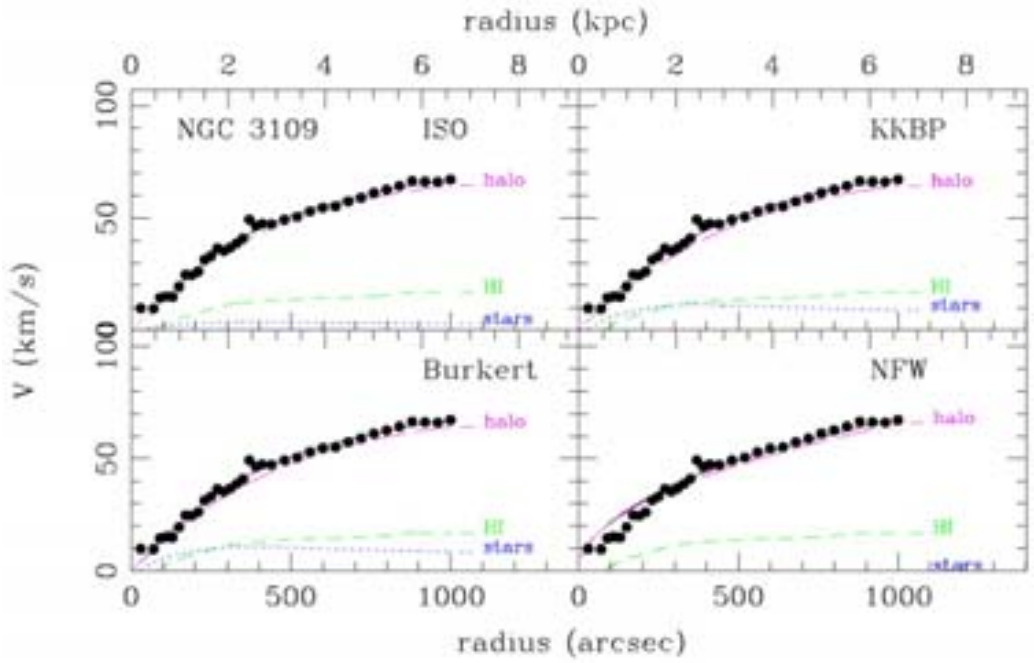

Fig. 8. Best-fit mass models for NGC 3109. Black dots: data derived from FP spectroscopy and HI. Models show dark matter halo density profiles for: pseudoisothermal sphere (top left), KKBP (top right), Burkert (bottom left) and NFW (bottom right). From Blais-Ouellette et al. (2001).

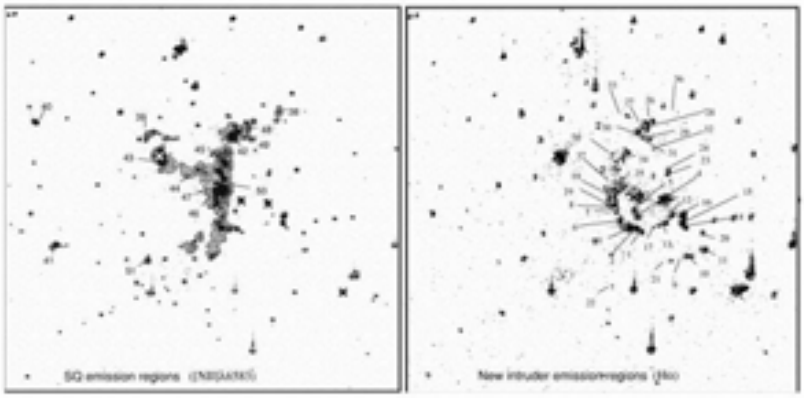

Fig. 9. Stephan Quintet's emission line regions (left) and new intruder's emission line regions (right), obtained from PUMA FP spectroscopy. From Sulentic et al. (2001).

existence of noncircular and random motions that preclude the discrimination between the halo distributions predicted by different models.

3.5. *Compact groups of galaxies*

Compact groups of galaxies (CGs) are small and relatively isolated aggregates of 4 to 8 galaxies whose mean separation is about a galactic diameter. They are among the most densest systems because their density is as high as the density of galaxy clusters' cores. CGs would constitute a link in the process of galaxy fusion. They are the highest cusps of the large-scale structure not located in galaxy clusters.

CGs are excellent laboratories to study the extreme effects of interactions. If interactions were more frequent in the past, then, the samples of nearby CGs constitute an important database to interpret observations at high redshifts.

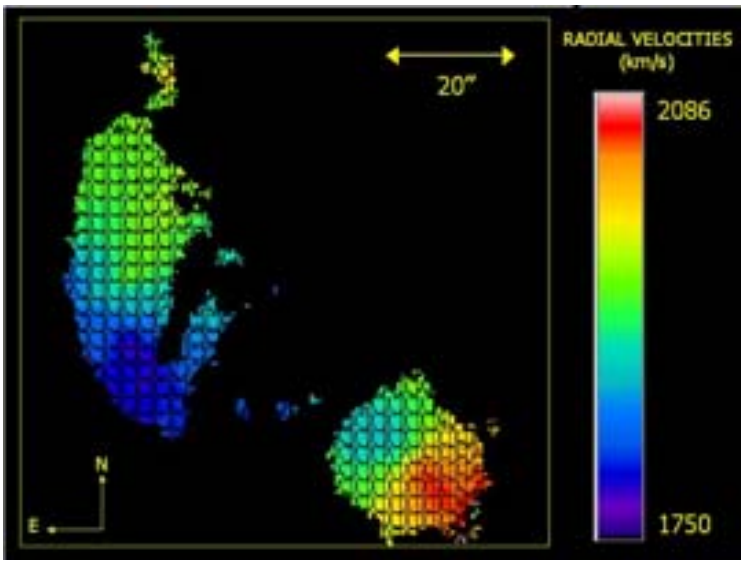

Fig. 10. PUMA [NII] velocity profiles superimposed on the radial velocity field of the galaxy pair KGP 468. From Hernández-Toledo et al. (2003).

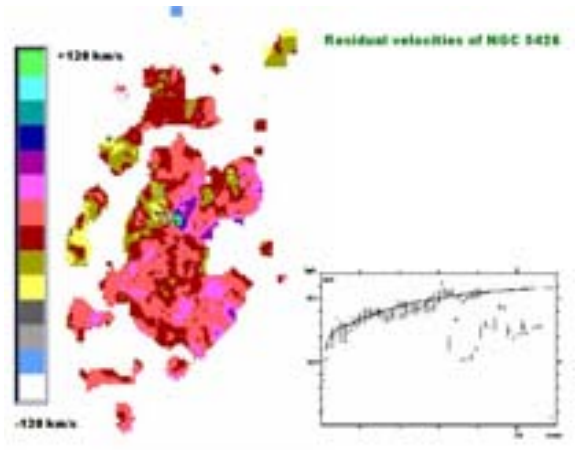

Fig. 11. Residual velocities of the galaxy NGC 5426, one of the members of the galaxy pair Arp 271. Bottom right: The fit to the rotation curve from which the circular velocities were subtracted from the observed velocity field. From Fuentes-Carrera et al. (2004).

FP interferometers are quite well suited to study CGs because the 2D kinematic data obtained with FPs could help in finding evidence of mergings and frequent and strong interactions within the members, in the reconstruction of their evolutionary history and in the identification of tidal dwarf galaxies, presumably formed by the interaction, to cite some of the several issues that can be studied in these objects.

Tidal dwarf galaxy candidates have been proposed for several CGs. For instance, the identification of tidal dwarf candidates in the most known of the CGs, the Stephan Quintet, was done by using the Fabry-Perot CIGALE at the CFHT by Mendes de Oliveira et al. (2002). However, the demonstration that the candidates are really tidal dwarfs instead of large HII complexes must await to obtain very high spatial and spectral resolution data, a project that could be done in telescopes as the GTC equipped with 3D spectrometers.

Regarding the Stephan Quintet, Figure 9 shows the different gaseous regions associated with this compact group and with the recent intruder, based on their velocities (Sulentic et al. 2001). This has been done from the kinematics obtained with PUMA at the OAN. For this particular case, the evolutionary history could be reconstructed.

3.6. *Interacting galaxy pairs*

These are the simplest cases of galaxy interactions. For these systems one expects that the interactions cause some degree of asymmetry and, consequently, 3D spectroscopy is ideal for studying the kinematics of interactions and to confront them with numerical simulations.

There are some works on isolated galaxy pairs, recently published, aimed at understanding the interaction process. These works were done using PUMA at the OAN.

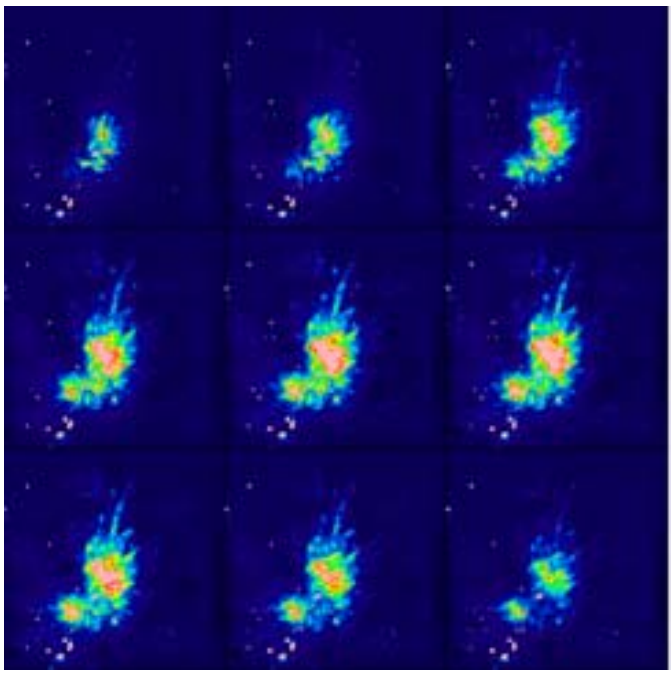

Fig. 12. PUMILA velocity maps of the molecular hydrogen emission at 2.12 μm of the Orion's OMC region. The difference in velocities between consecutive maps is about 10 km s^{-1}; the FOV $\sim 4'.5$. The Orion fingers are clearly seen. From Salas et al. (1999).

Figure 10 shows the [NII] radial velocity profiles of the galaxy pair KGP 468, superimposed on the radial velocity field of this system (Hernández-Toledo et al. 2003). The bridge and the tidal tails are clearly seen as well as the complexity of some of the velocity profiles even for the early-type galaxy member located at the SW. In these systems one also expects that the members' gas undergo strong deviations to circular motions. Indeed, this seems to be the case for NGC 5426, one of the members of another galaxy pair, Arp 271 (Fuentes-Carrera et al. 2004). Figure 11 shows the 2D residual velocities of Arp 271 that allowed us to know the precise geometry of the encounter. These results are important in order to establish boundary conditions for dynamical modeling of galaxy interactions.

4. 3D SPECTROSCOPY IN THE NEAR INFRARED

The results outlined above were obtained in the optical range of the spectrum. However, the use of 3D spectrometers in the near IR is quite appealing because the data obtained with those instruments would be unique in a series of problems, for example:

– Kinematics of the molecular gas, by means of obtaining velocity cubes in the line at 2.12μm of the molecular hydrogen. This technique could be applied to star forming regions and Herbig-Haro objects in our Galaxy and in other galaxies, to planetary nebulae and to low metallicity galaxies and starbursts, amongst several objects.

– Kinematics of the ionized gas in highly reddened nuclei.

– Kinematics of highly redshifted objects.

The instruments of this kind are scarse in spite that the studies in the near IR open a new view of our Universe that waits to be explored.

We have developed a prototype which uses a scanning Fabry-Perot interferometer optimized in the near IR (PUMILA). This instrument is working at the 2.1m telescope of the OAN. It has been used to obtain velocity-cubes of the line at 2.12μm of the molecular hydrogen, corresponding to the v = 1-0 rotational transition with a sampling velocity resolution of 10 km s^{-1} (see Rosado et al. 1999, Arias et al. 2001).

Figure 12 depicts the velocity maps of the molecular hydrogen in the Orion's OMC region showing what is known as the "fingers" (Salas et al. 1999). The fingers are directly associated with Herbig-Haro objects (that are defined only by their optical properties).

In the case of planetary nebulae, the velocity

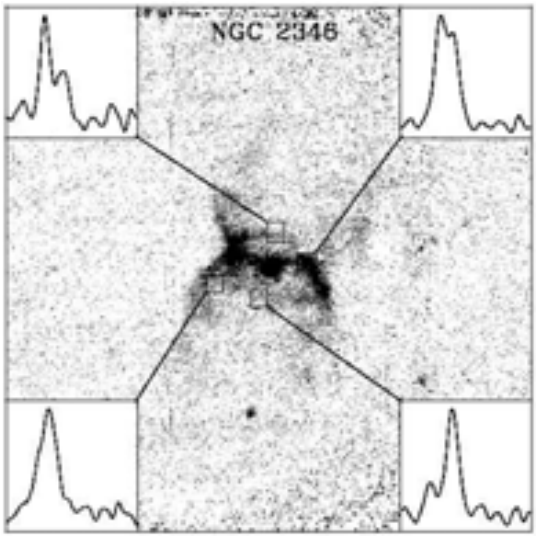

Fig. 13. Typical radial velocity profiles of the molecular gas in NGC 2346 in the H_2 line at 2.12μm superimposed on a direct image in the same line at 2.12μm (from Arias et al. 2001).

maps of the molecular hydrogen have been revealed as very useful in the identification of the mechanism that excites the line at 2.12μm, as well as in the determination of the mass and evolution of these objects. Figure 13 shows typical radial velocity profiles of the H_2 emission line at 2.12μm superimposed on the image of NGC 2346 emission at 2.12μm. Since our FP velocity cubes allow us to obtain radial velocity profiles of each pixel over the whole extension of this PN, we are able to obtain position-velocity diagrams that could be used to fit a geometrical model (Arias et al. 2001). Supersonic motions of the molecular hydrogen were found in this object implying that shocks excite this emission.

5. CONCLUSIONS

I have given an overview of interesting results obtained with data from 3D spectrometers at 4m-class telescopes. One can extrapolate and draw the following conclusions:

– Many scientific niches will be exploited by means of 3D spectrometers in 8–10m-class telescopes (for example, OSIRIS in the GTC).

– 3D spectrometers and adaptive optics are the best combination to exploit the high spatial resolution provided by adaptive optics systems.

– 3D spectrometers in large telescopes working in the near IR will reveal another view of the Universe.

MR wishes to thank the SOC and LOC of this nice meeting for the invitation. She also wishes to acknowledge the financial support from grants IN120802 of DGAPA-UNAM and 2002-C01-40095 of CONACYT.

REFERENCES

Arias, L., et al. 2001, AJ, 122, 3293
Bacon, R., et al. 2001, A&A, 371, 409
Blais-Ouellette, S., et al. 2001, AJ, 121, 1952
Cecil, G., et al. 2001, ApJ, 576, 745
Connes, P. & Le Coarer, E. 1995, ASP Conf. Series, 71, 38
de Zeeuw, P. T., et al. 2002, MNRAS, 329, 513
Emsellem, E., et al. 1999, MNRAS, 303, 495
Fuentes-Carrera, I. 2004, A&A, 415, 451
Hernández-Toledo, H., et al. 2003, A&A, 412, 669
Mediavilla, et al. 1998, ApJ, 503, L27
Mendes de Oliveira, C., et al. 2002, AJ, 121, 2524
Melo, V., et al. 2003, RMxAC, 16, 298
Miller, S.T. & Veilleux, S. 2003, ApJS, 148, 383
Rand, R.J. 1996, ApJ, 462, 712
Reynolds, R.J. 2002, ASP Conf. Series, 282, 31
Rosado, M., et al. 1999, in Proc. SPIE, 3354, 1111
Rosado, M., et al. 2002, AJ, 122, 194
Salas, L., et al. 1999, ApJ, 511, 822
Sulentic, J. W. 2001, AJ, 122, 2993
Swaters, R.A., et al. 2003, ApJ, 587, L19
Valdez-Gutiérrez, M., et al. 2001, A&A, 366, 35
Valdez-Gutiérrez, M., et al. 2002, AJ, 124, 3157
Veilleux, S. 2004, this issue
Veilleux, S., et al. 1995, ApJ, 445, 152
Zurita, A., et al. 2000, A&A, 363, 9

Margarita Rosado: Instituto de Astronomía, UNAM, Apdo. Postal 70-264, México, D.F. CP 04510 México (margarit@astroscu.unam.mx).